Available online www.jocpr.com

Journal of Chemical and Pharmaceutical Research, 2015, 7(5):246-259

Research Article

ISSN : 0975-7384
CODEN(USA) : JCPRC5

Synthesis, characterization, single crystal XRD and pharmacological evaluation of Cu(II), Co(II), Ni(II) and Zn(II) complexes of 2,3-difurylquinoxaline

S. Jone Kirubavathy[a], R. Velmurugan[a], K. Parameswari[b] and S. Chitra[b]*

[a]*Department of Chemistry, Kongunadu Arts and Science College, Coimbatore*
[a]*Department of Chemistry, P. S. G. R. Krishnammal college for women, Coimbatore*

ABSTRACT

The transition metal complexes Cu(II), Co(II), Ni(II) and Zn(II) of 2, 3-difuryl quinoxaline have been synthesized and characterized by various physico-chemical techniques viz. elemental analysis, magnetic moment, IR, NMR, TGA, Single crystal XRD and electronic studies. The complexes have found a stoichiometry of 1:2 (M : L), wherein nitrogen in the quinoxaline ring and oxygen in the furyl ring is co-ordinated to the metal. These studies revealed an octahedral geometry for Cu(II) and Co(II) complexes and a square planar geometry for Ni(II) and Zn(II) complexes. The ligand and its complexes were screened for their antibacterial activity against gram positive bacteria and gram negative bacteria namely B. subtilis, S. aureas, E. coli , K. pneumoniea respectively by the disc diffusion method and antifungal activity against M. rubram, A. niger and C. albicans and found to be good. The in-vitro anti cancer activity of the single crystal 2, 3-difurylquinoxaline and its Co(II) complex was screened against the human breast cancer cell line HeLa and the IC_{50} values are 90.19 and 20.25µg/ml respectively.

Keywords: 2,3- difuryl quinoxaline, Single crystal XRD, transition metal complexes, breast cancer, anti-microbial.

INTRODUCTION

Quinoxaline derivatives are well known in the pharmaceutical industry and have been shown to possess a broad spectrum of biological activities including anti-viral[1], anti-bacterial[2], anti-inflammatory[3], anti-cancer[4] and anthelmintic[5] agents. Chloroquine a traditional old antimalarial drug is believed to exert its activity by inhibiting hemozoin formation in the digestive vacuole of the malaria parasite, but the mechanism of *Plasmodium falciparum* resistant to chloroquine remains unknown. Recently, some pyrrolo-quinoxaline derivatives have shown antimalarial activity correlated with a high inhibitory of β-hematin formation[6]. Quinoxaline derivatives are a class of compounds that show very interesting biological properties and the interest in these compounds is growing within the field of medicinal chemistry. The transition metal complexes of quinoxaline derivatives and their pharmacological activity remains unexplored and the aim of this present investigation is to synthesis metal complexes of 2, 3-difurylquinoxaline and explore their biological activity.

EXPERIMENTAL SECTION

All reagents, 1, 2-diketone, o-phenylenediamine metal chloride/nitrates were purchased from Sigma Aldrich, India.

2.2. Physical Measurements

2.2. Instrumentation

Microanalytical data of the compounds were recorded in the *ElementarVario EL III* CHN Analyser. Metal estimations were determined complexometrically by standard EDTA titration. The FT-IR spectra of the samples were recorded on a *Shimadzu* spectrophotometer in 4000-400 cm^{-1}.^{1}H NMR(300 MHz) and ^{13}C NMR (400 MHz) were recorded using *Jeol* 400 MHz Spectrometer with DMSO $-d^6$ was used as a solvent and TMS as an internal standard. The UV-Visible spectra were recorded on an *Elico SL 159* UV-Vis Spectrophotometer. Magnetic susceptibility measurements of the complexes were carried out by *Guoy balance* using copper sulphate as the calibrant. The magnetic susceptibility of the metal complexes were calculated using the relation $\mu_{eff}=2.828(\chi_m.T)^{1/2}BM$ where χ_m is the molar susceptibility corrected using Pascal's constants for diamagnetism of all atoms in the compounds. The molar conductance of the complexes was measured using a S*ystronics* conductivity bridge at room temperature in DMSO solution. The thermal behavior of the complexes was studied using Perkin *Elmer STA 6000*thermoanalyser. EPR spectrum of Cu(II) complex was recorded at room temperature on an *ESR-JEOL-12* spectrometer using the DPPH as the g-marker. The antimicrobial activities of the ligand and its complexes were carried out by disc diffusion method. The *in-vitro* anticancer activity were carried out using MTT assay.

2.3. Synthesis of ligand

o-phenylenediamine and furil were dissolved in the mixture of solvents (ethanol/water (1:1)). A catalytic amount of iodine was added and the mixture was kept in microwave oven and irradiated for three minutes using microwave oven (Scheme.1). The reaction was monitored by TLC. After completion of the reaction, dichloromethane (10 mL) was added to the reaction mixture and it was then washed successively with 5% sodium thiosulphate solution (2 mL) and brine (2 mL). The organic layer was dried with anhydrous sodium sulphate and concentrated. No column chromatography was needed for the purification of the products and pure products were isolated through crystallization by using the solvent mixture dichloromethane-hexane [7]

Scheme 1: Synthesis of 2, 3-difurylquinoxaline

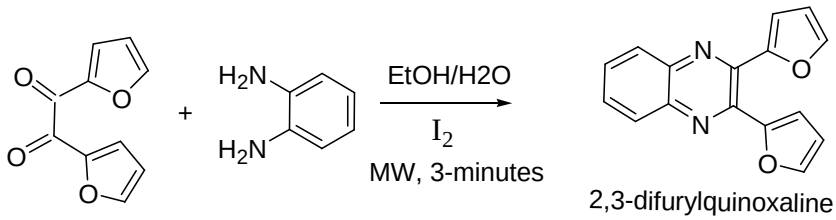

2.4. Synthesis of complexes

An ethanolic solution of metal chloride/nitrate and 2, 3-difurylquinoxaline were refluxed for 5h. After completion of the reaction, the complexes (Scheme 2) obtained was filtered, washed with ether and dried.

2.5. Determination of X-Ray crystal structure of 2,3-difurylquinoxaline

X-ray diffraction for the ligand 2,3-difurylquinoxaline was made on a *Bruker APEX CCD-II* area detector diffractometer with graphite monochromated*Mo-Kα* radiation (λ = 0.71073 Å). The crystal structure was solved by direct methods. Structure refinements were performed by full matrix least squares procedures using SHELXL-97 on F^2 [8, 9]

2.6. Antimicrobial activity

The antibacterial activity of the ligand and the metal complexes were screened for gram positive bacteria and gram negative bacteria namely *B.subtilis, S. aureas, E. coli, K. pneumoniea* respectively by the disc diffusion method using agar nutrient as the medium. The antifungal activities were screened for the organisms *M. rubram, A. niger* and *C. albicans* by the disc diffusion method cultured on potato dextrose agar as medium. The plate was incubated 24h for bacteria and 72h for fungi. During this period, the test solution diffused and the growth of the inoculated microorganisms was affected. The inhibition zone was developed, at which the concentration was noted [10-12].

2.7. Anticancer activity- Cell treatment procedure and MTT assay

The monolayer cells were detached with trypsin-ethylenediaminetetraacetic acid (EDTA) to make single cell suspensions and viable cells were counted using a hemocytometer and diluted with medium containing 5% FBS to

give final density of 1×10^5 cells/mL. Cell suspensions were seeded into 96-well plates at plating density of 10,000 cells/well and incubated to allow for cell attachment at 37°C. After 24 h, the cells were treated with serial concentrations of the test samples. They were initially dissolved in DMSO and diluted to twice the desired final maximum test concentration with serum free medium. Additional four, 2 fold serial dilutions were made to provide a total of five sample concentrations. Aliquots of 100 µL of these different sample dilutions were added to the appropriate wells already containing 100 µL of medium, resulted the required final sample concentrations. Following drug addition, the plates were incubated for an additional 48 h at 37°C. The medium containing without samples was served as control and triplicate was maintained for all concentrations.

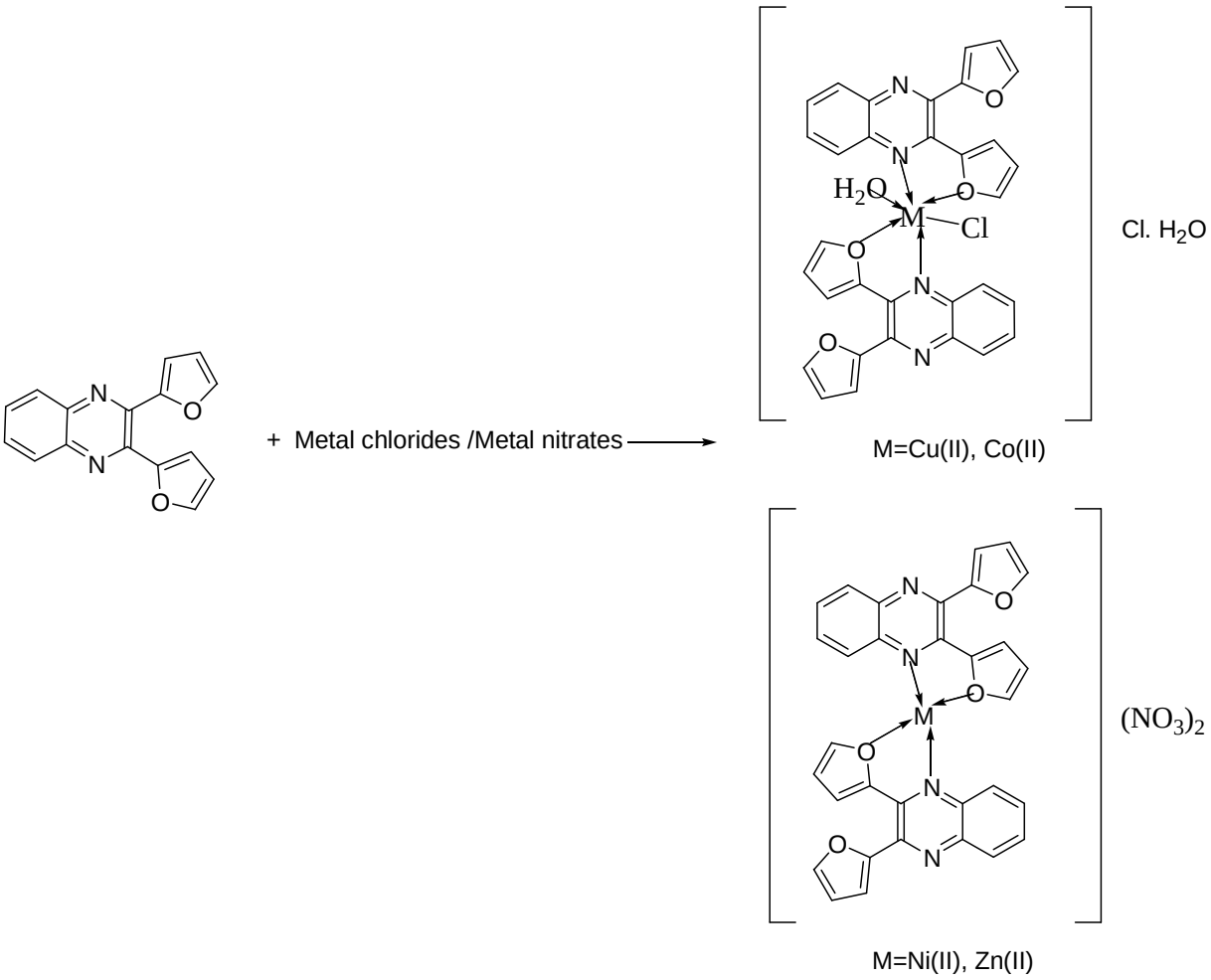

3-[4,5-dimethylthiazol-2-yl]2,5-diphenyltetrazolium bromide (MTT) is a yellow water soluble tetrazolium salt. A mitochondrial enzyme in living cells, succinate-dehydrogenase, cleaves the tetrazolium ring, converting the MTT to an insoluble purple formazan. Therefore, the amount of formazan produced is directly proportional to the number of viable cells. After 48 h of incubation, 15 µL of MTT (5 mg/mL) in phosphate buffered saline (PBS) was added to each well and incubated at 37°C for 4 h. The medium with MTT was then flicked off and the formed formazan crystals were solubilized in 100 µL of DMSO and then measured the absorbance at 570 nm using micro plate reader. The % cell inhibition was determined using the formula, % cell Inhibition = 100 – Abs (sample)/Abs (control) × 100. Nonlinear regression graph was plotted between % cell inhibition and $\log_{10}$ (concentration) and IC_{50} was determined using graph pad prism software.

RESULTS AND DISCUSSION

3.1. The Ligand

2,3-difurylquinoxaline(Figure 1) is formed via the condensation of the diketone and 1, 2-diamine. The analytical data of the ligand is in good agreement with those of the calculated formula(Table 1).

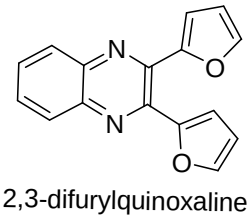

2,3-difurylquinoxaline

Figure 1. The structural diagram of the ligand

The ^{1}H NMR spectrum of the ligand(Figure 2) 2,3-difurylquinoxaline revealed its formation by the presence of aromatic protons in the quinoxaline ring at δ 7.9 and δ 8.1 ppm. The signals at δ 6.7 and δ 7.8 ppm corresponds to the protons in the furyl ring attached to the quinoxaline moiety.

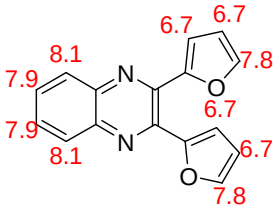

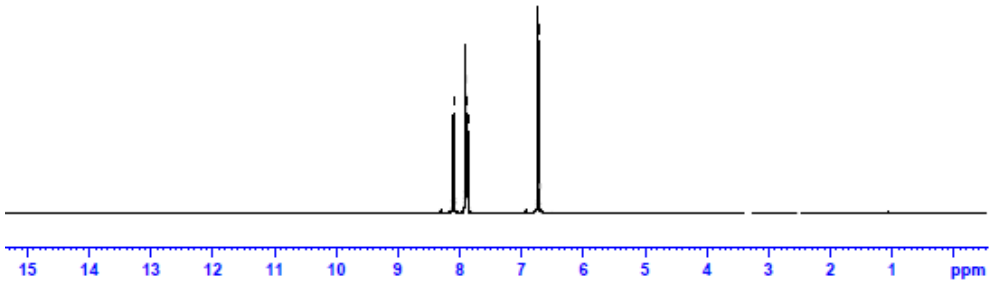

Figure 2. ^{1}H NMR Spectrum of the ligand 2,3-difurylquinoxaline

The chemical shifts for carbons of (-N=C-) in the quinoxaline ring was observed at 142 ppm. The signal observed at 144.9 ppm corresponds to the carbon where the furyl is attached. The spectrum showed peaks at 112.8-150.3ppm and 128.6-130.8 ppm corresponding to carbons of the furyl and phenyl ring respectively.The ^{13}C NMR spectrum of the ligand is shown in Figure 3.

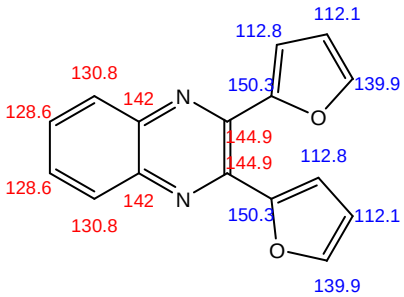

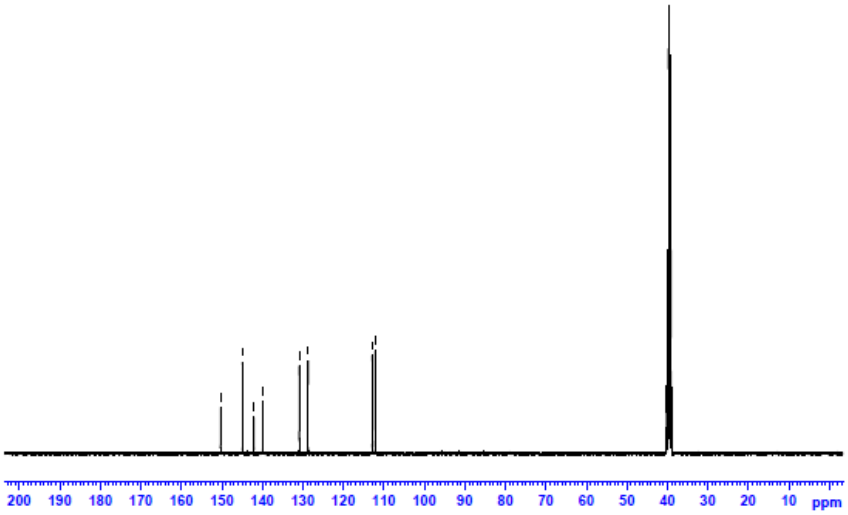

Figure 3. ^{13}C NMR Spectrum of the ligand 2,3 -difurylquinoxaline

Single Crystal X-Ray studies of 2, 3-difuryl quinoxaline($C_{16}H_{10}N_2O_2$) confirms its structure. It crystallises in orthorhombic space group Pna21 with the unit cell dimensions a = 15.6578 (13)Å, b = 16.8802 (12)Å, c = 4.6970 (3)Å, Z = 4. The crystal structure was solved by direct methods and refined by full matrix least squares procedures to a final R value of 0.0372 with 3009 observed reflections. The crystal has a volume of 1241.45(16)Å^3. The ORTEP diagram of the ligand 2, 3-difurylquinoxaline is shown in Figure 4.

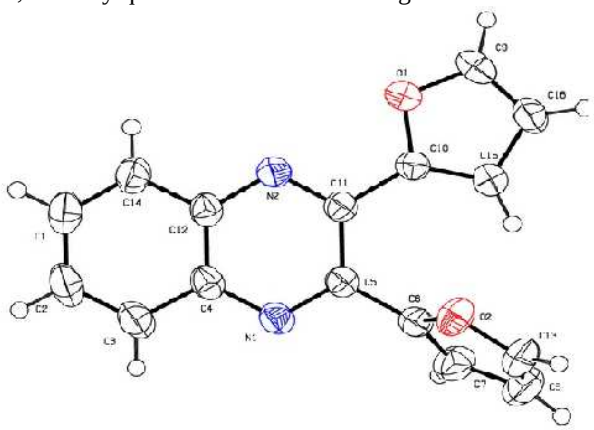

Fig. 4 ORTEP diagram of the ligand 2, 3-difurylquinoxaline

Further insight concerning the structure of the ligand is obtained from IR and UV-Visible measurements which will be discussed with its metal complexes.

3.2. Metal Complexes

The chemical behaviour of the ligand towards transition metals like Co(II), Ni(II), Cu(II) and Zn(II) were studied. When a mixture of the ligand 2, 3-difurylquinoxaline and metal chlorides/nitrates in ethanol were made to react, a change in colour was observed and the complex gets precipitated. The products were purified and gave elemental analyses compatible with the suggested formulae given in Table 1. On the basis of the elemental analysis data(Table 1), all the complexes have the general composition $[ML_2(OH_2)Cl]Cl.H_2O$ where M=Co, Cu and $[ML_2](NO_3)_2$ where M=Ni(II), Zn(II). The obtained complexes are powder solids which are stable in air and decompose above 300°C. The confirmation of the proposed structures of the ligand 2, 3-difurylquinoxaline with the metal salts was done using different physic-chemical methods shown below.

Table 1: Analytical data of the ligand 2,3-difurylquinoxaline and its complexes

Compound	M	C	H	N	Λ_m	Mol. W
$C_{16}H_{10}N_2O_2$	-	73.27(73.26)	3.84(3.80)	10.68(10.65)	-	262.26
$[CuL_2(OH_2)Cl]Cl.H_2O$	9.14(9.11)	55.30(55.29)	3.48(3.51)	8.06(8.04)	94.3	695.01
$[CoL_2(OH_2)Cl]Cl.H_2O$	8.54(8.57)	55.67(55.69)	3.50(3.53)	8.12(8.13)	89.5	690.40
$[NiL_2](NO_3)_2$	9.10(9.12)	59.57(59.56)	3.12(3.15)	10.85(10.84)	105.1	645.22
$[ZnL_2](NO_3)_2$	10.03(10.07)	58.96(58.93)	3.09(3.10)	10.74(10.77)	112.6	651.92

3.2.1. Molar Conductivities of metal complexes

Molar conductance measurements of the complexes carried out using DMF as solvent at the concentration of 10^{-3}M, indicating electrolytic behavior of the complexes and conductivity values were found in the range 84-120$\Omega^{-1}cm^2mol^{-1}$[13].

3.2.2. IR spectra and mode of binding

The infrared spectra assignment of the proposed structures of the complexes was made through consideration of the infrared spectra. The IR spectra of the free ligand and metal complexes (Table 2) were carried out in the range 4000-400cm^{-1}. The IR spectrum of the ligand shows a peak at 1648cm^{-1} which corresponds to $\gamma_{C=N}$ in the quinoxaline ring, γ_{C-O} in the furyl ring appears at 1148 cm^{-1}. On complexation, there are two types of $\gamma_{C=N}$ found one co-ordinated and the other remains unco-ordinated. The stretching frequency of the $\gamma_{C=N}$ in the quinoxaline ring which is co-ordinated to the metal is shifted to lower frequencies 1600cm^{-1} to 1634cm^{-1} and there is a band at and around 1648cm^{-1} which corresponds to $\gamma_{C=N}$ in the quinoxaline ring that is not co-ordinated to the metal. This proves that there are two types of $\gamma_{C=N}$ present in the complex one is co-ordinated to the metal and the other remains unco-ordinated. Likewise the C-O in the furyl ring shifts to lower frequencies 1111 cm^{-1} to 1143 cm^{-1}. From IR spectra it is proved that the co-ordination sites are 'N' in the quinoxaline ring and 'O' in the furyl ring [14, 15]. This can be visualized much better in the atom numbering scheme from single crystal XRD of the ligand where N2 and O1 are found to be the co-ordination sites and not N1 and O2 which are found to be in different plane.

The infrared wavenumbers(cm^{-1}) and tentative band assignments for the synthesized ligand(2,3-difuryl quinoxaline) and its metal complexes are given in Table 2. The bands around 3300cm^{-1} in Cu(II) and Co(II) complexes shows the presence of water in the complex. The thermal gravimetric studies also proves its nature of water molecule as lattice or co-ordinated. In the far IR spectra of all the complexes, the non-ligand bands observed at 450-465cm^{-1} region assigned to γM-N stretch. Conclusive evidence regarding the bonding of oxygen to the metal ions is provided by the occurrence of bands at 504-517cm^{-1} region due to γM-O.

Table 2. The infrared wavenumbers(cm^{-1}) and tentative band assignments for the synthesized ligand(2,3-difuryl quinoxaline) and its metal complexes

Compound	γH_2O	$\gamma C=N_{co\text{-}ord}$	$\gamma C=N_{unco\text{-}ord}$	$\gamma C\text{-}O_{co\text{-}ord}$	$\gamma C\text{-}O_{unco\text{-}ord}$	γM-N	γM-O
$C_{16}H_{10}N_2O_2$	-	-	1648	-	1148	-	-
$[CuL_2(OH_2)Cl]Cl.H_2O$	3333	1634	1647	1137	1148	451	504
$[CoL_2(OH_2)Cl]Cl.H_2O$	3300	1604	1648	1117	1147	450	513
$[NiL_2](NO_3)_2$	-	1627	1648	1143	1147	446	514
$[ZnL_2](NO_3)_2$	-	1635	1647	1128	1148	465	517

3.2.3. Electronic spectral data

The free ligand displayed absorption bands at 220 and 280nm. The shorter wavelength band is attributed to the high energy π-π* transition and the longer wavelength band was assigned to the n-π* transition within the C=N group. The observed magnetic moment of the Cu(II) complex is 1.79 BM and the electronic spectrum of the complex displays bands at 750nm, 580nm and 460nm which may be assigned to $^2B_{1g}\rightarrow{}^2A_{1g}$ (υ1),$^2B_{1g}\rightarrow{}^2B_{2g}$(υ2) and $^2B_{1g}\rightarrow{}^2E_g$ respectively confirming the tetragonally distorted octahedral environment around the Cu(II) ion. Co(II) complex shows magnetic moment at 3.94 B. M. corresponding to three unpaired electrons. The electronic spectrum of the Co(II) complex displays three bands at 790nm, 650nm and 405 nm. These bands may be assigned to the following transitions $^4T_{1g}\rightarrow{}^4T_{2g}$(F)(υ1), $^4T_{1g}\rightarrow{}^4A_{2g}$(F)(υ2) and $^4T_{1g}\rightarrow{}^4T_{1g}$(P)(υ3) respectively. The position of the bands suggest octahedral geometry of Co(II) complex. The electronic absorption spectra of Ni(II) complex consists of two bands at 580nm and 389nm assignable to $^1A_{1g}\rightarrow{}^1T_{2g}$and charge transfer transitions respectively. Observed transitions and the diamagnetic nature(μ=0) of the complex suggests square planar geometry for Ni(II) complex[16, 17]. The observed magnetic moment and the electronic spectral data of the complexes are given in Table 3. The proposed geometry of the complexes and their 3D view are given in Figure 5 and 6.

Table 3. The observed magnetic moment and the electronic spectral data of the complexes

Compound	Geometry	μ_{eff}	Band assignments	λ_{max}(nm)
$C_{16}H_{10}N_2O_2$	-	-	n-π*, π-π*	280 220
$[CuL_2(OH_2)Cl]Cl.H_2O$	Octahedral	1.79	$^2B_{1g}\rightarrow{}^2A_{1g}((\upsilon 1)$, $^2B_{1g}\rightarrow{}^2B_{2g}(\upsilon 2)$ $^2B_{1g}\rightarrow{}^2E_g$	750 580 460
$[CoL_2(OH_2)Cl]Cl.H_2O$	Octahedral	3.94	$^4T_{1g}\rightarrow{}^4T_{2g}(F)(\upsilon 1)$ $^4T_{1g}\rightarrow{}^4A_{2g}(F)(\upsilon 2)$ $^4T_{1g}\rightarrow{}^4T_{1g}(P)(\upsilon 3)$	790 650 405
$[NiL_2](NO_3)_2$	Square Planar	0	$^1A_{1g}\rightarrow{}^1T_{2g}$ Charge Transfer	580 389

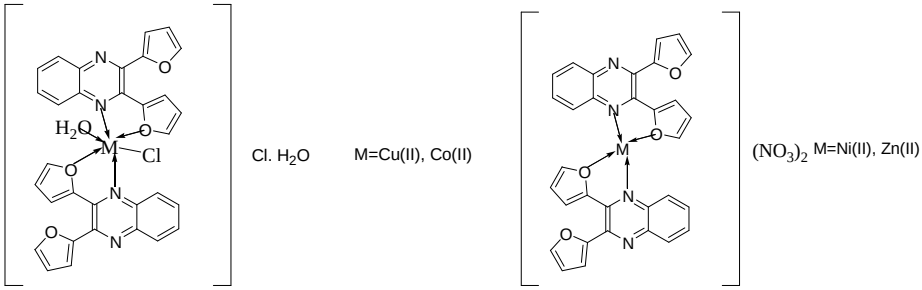

Figure 5. The proposed geometry of the complexes

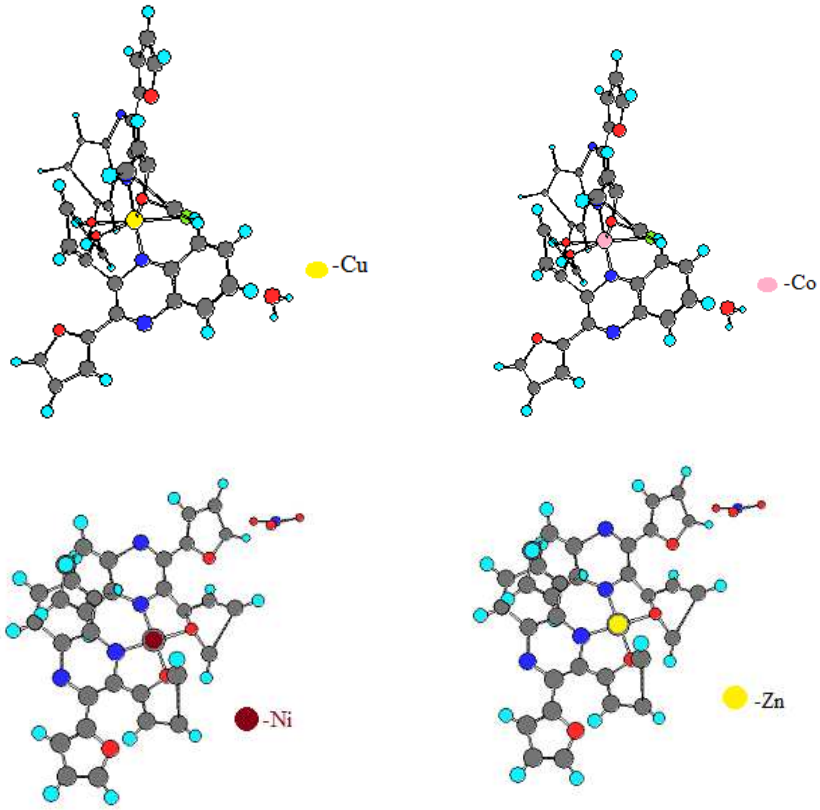

Figure 6. 3D view of the complexes

3.2.4. NMR Spectral data of Zn(II) complex

Comparing the NMR spectral data of the ligand and the Zn(II) complex, the values of the carbon and hydrogen are deshielded which proves the formation of the complex. The ^{1}H NMR and ^{13}C NMR spectrum of Zn(II) complex is shown in Figure 7 and 8 respectively.

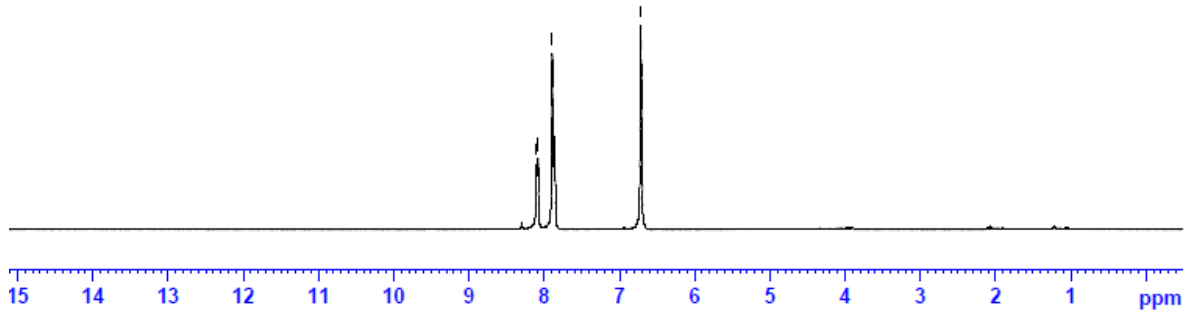

Figure 7. ^{1}H NMR SPECTRUM OF Zn(II) COMPLEX

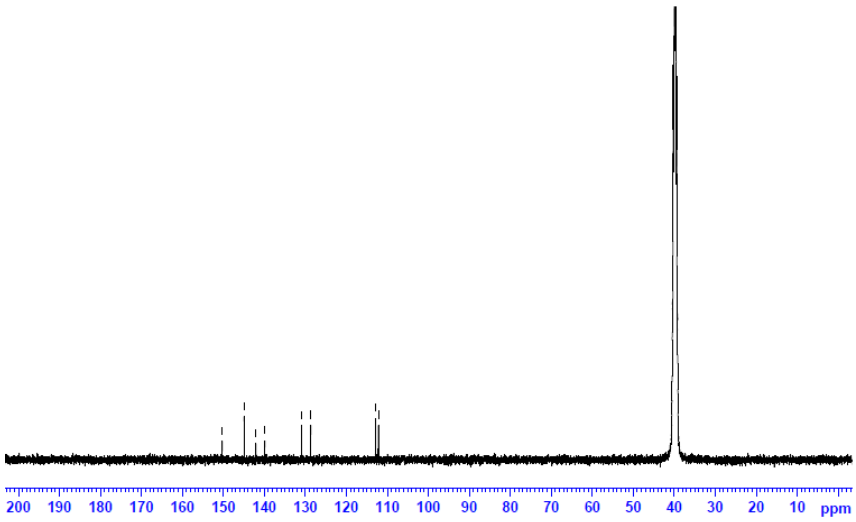

Figure 8. ^{13}C NMR spectrum of Zn(II) complex

3.2.5. ESR Spectral Data of [$CuL_2Cl(H_2O)$]Cl. H_2O complex

g value of Cu(II) complex can be used to derive the ground state. In elongated octahedral and square planar complexes, the unpaired electron lies in the dx^2-y^2 orbitals giving $^{2}B_{1g}$ as the ground state with $g_{11} > g_{\perp}$. The low temperature EPR spectra of present complex(Fig. 9) is the indication of dx^2-y^2 ground state ($g_{11} > g_{\perp} > 2.03$) and thus suggest a dominally tetragonal component. The analysis of spectra give g_{11}=2.33 and $g_{\perp}$=2.09. The trend $g_{11} > g_{\perp} > 2.03$ is observed for the complex under study indicates that the unpaired electron is localized in d_{x2-y2} orbital of the Cu(II) ion and the spectral features are characteristic for axial geometry. Tetragonal elongated geometry is thus confirmed for the above complex [18, 19]. The ESR spectrum of the complex is shown in Figure 9.

Table 4. ESR parameters of [$CuL_2Cl(H_2O)$]Cl.H_2O complex

Complex	g_{11}	$g_{\perp}$	A_{11} x10^{-4} cm^{-1}	g_{11}/A_{11} cm-1	G	α^2
[$CuL_2Cl(H_2O)$]Cl.H_2O	2.33	2.09	347	69	4.83	1.27

Figure 9. ESR spectrum of$[CuL_2Cl(H_2O)]Cl.H_2O$ complex

3.2.6. Thermal Analysis

The thermal degradation of the complexes were studied using thermogravimetric techniques and temperature range of 25-800°C. The thermal stability data are listed in Table 6. The data from the thermogravimeric analysis clearly indicated that the decomposition of the complexes proceeds in two or three steps. Water molecules were lost in between 50 and 200°C and metal oxides were formed above 600°C for all the complexes. In Cu(II) and Co(II) complexes, the removal of water can proceed in one or two steps. Cu(II) complex lost hydration water at 80.04°C and the co-ordinated water was lost at 169.64°C. Co(II) complex lost hydration water at 122.96°C. The decomposition was complete at ≥600°C for all the complexes. The decomposition steps with the temperature range and weight loss for all the complexes are given in Table 6 and the TGA/DTA spectrum of the complexes are given in Figure 10.

Table 6. The decomposition steps with the temperature range and weight loss for all the complexes

Compound	n*	T(°C)	Removed Fragments	Wt. Loss		Residue
				% Calcd.	% Found	
$[CuL_2(OH_2)Cl]Cl.H_2O$	I	35-100	$-H_2O$	02.58	02. 50	CuO
	II	150-250	$-H_2O$	02.58	02.49	
	III	260-700	$-2NH_3$, 2HCl, $C_{32}H_{12}$	72.36	72.25	
$[CoL_2(OH_2)Cl]Cl.H_2O$	I	35-150	$-2H_2O$	05.21	05.15	CoO
	II	200-700	$-2NH_3$, 2HCl, $C_{32}H_{12}$	67.56	67.45	
$[NiL_2](NO_3)_2$	I	35-700	All co-ordinated and uncoordinated part of the complex in a single step	91.66	91.76	NiO
$[ZnL_2](NO_3)_2$	I	35-700	All co-ordinated and uncoordinated part of the complex in a single step	88.76	88.54	ZnO

** number of decomposition steps*

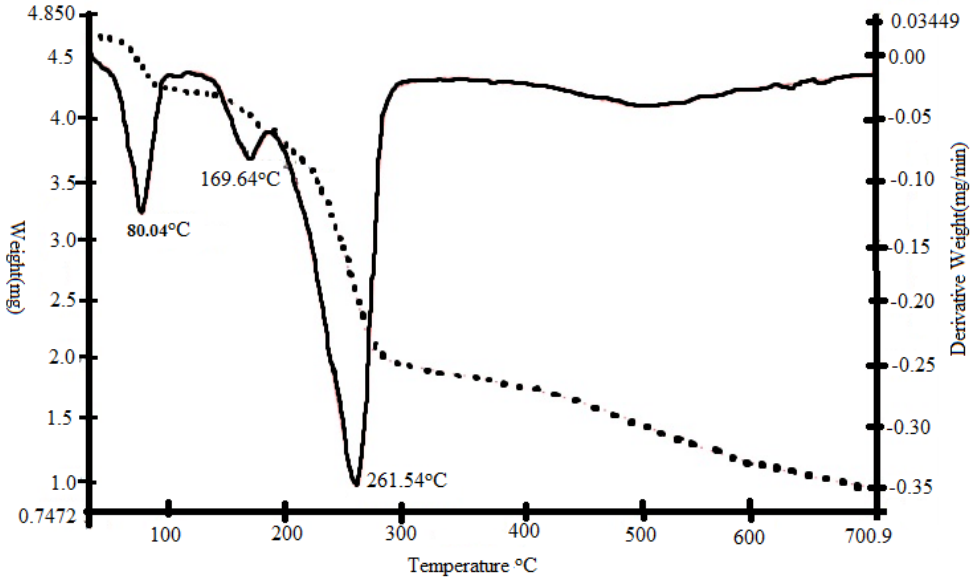
4.850
4.5
4.0
3.5
3.0
2.5
2.0
1.5
1.0
0.7472
Weight(mg)
0.03449
0.00
-0.05
-0.10
-0.15
-0.20
-0.25
-0.30
-0.35
Derivative Weight(mg/min)
80.04°C
169.64°C
261.54°C
100
200
300
400
500
600
700.9
Temperature °C

(a)

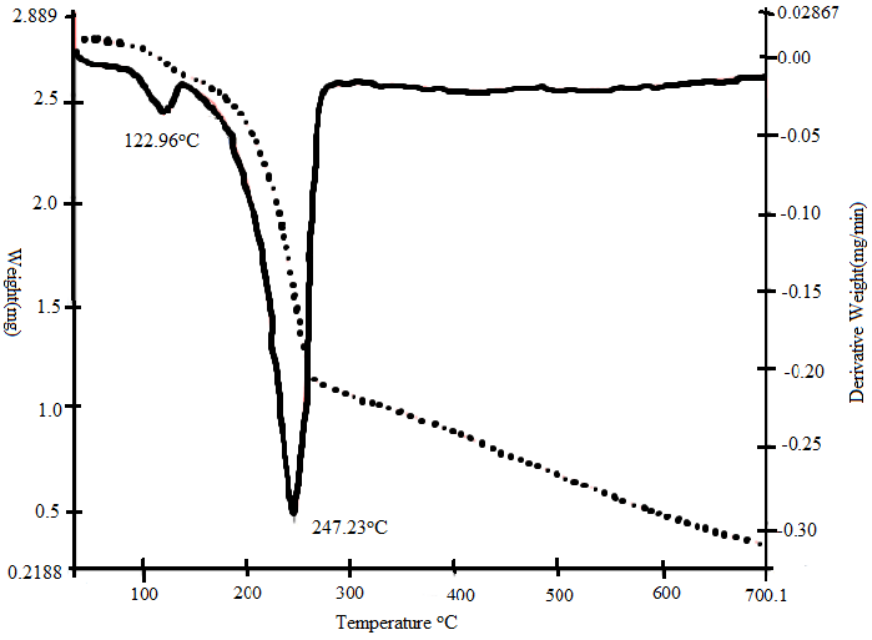
2.889
2.5
2.0
1.5
1.0
0.5
0.2188
Weight(mg)
0.02867
0.00
-0.05
-0.10
-0.15
-0.20
-0.25
-0.30
Derivative Weight(mg/min)
122.96°C
247.23°C
100
200
300
400
500
600
700.1
Temperature °C

(b)

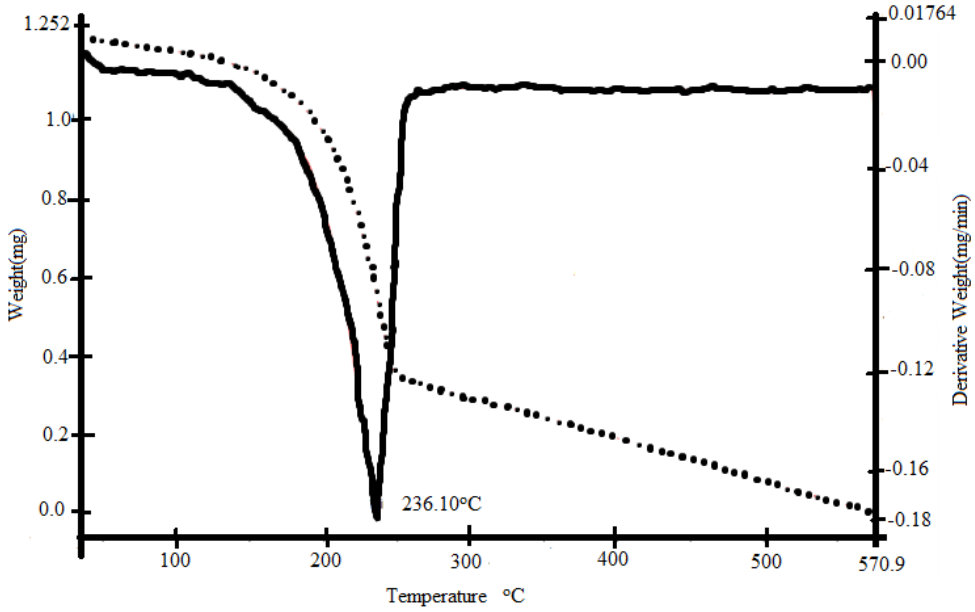

(c)

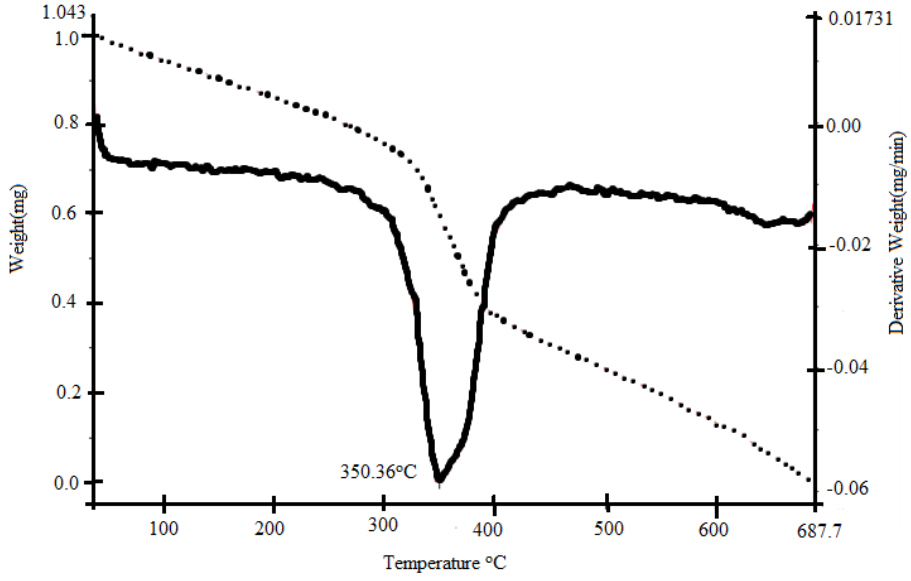

(d)

Figure 10. TGA/DTA spectrum of a)Cu(II) b) Co(II) c) Ni(II) d)Zn(II) complexes

4. Pharmacology

4.1. Antibacterial activity

The results of the antimicrobial activities are summarized in Table 7 and 8. DMSO is used as the negative control and amikacin, Ofloxacin and ciprofloxacin were used as the positive standards for antibacterial studies. Nystatin was used as a reference for antifungal activities. These compounds exhibit moderate to strong antimicrobial activity. Comparitively a better activity is found for bacteria rather than fungi. The copper complex shows a very good activity than the other complexes especially for the test organism *B. subtilis*. Only the activity of Zinc complex is moderate. The antifungal activity of the complexes are also very good. The nickel complex shows a very good activity against *M. rubram* and *A. niger*. The activity of the other complexes are also good and more than that of the ligand and the test standard in most of the cases. The increased activity of the complexes comparing the ligand can be explained based on the Overtone's concept and Tweedy's chelation theory [20, 21].

Table 7: Antibacterial screening of the ligand and the complexes

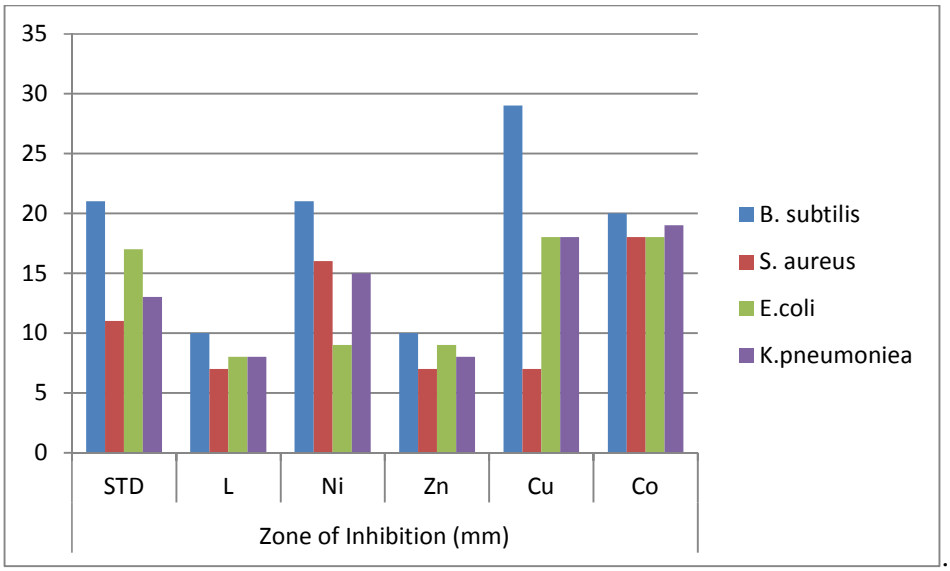

Table 8: Antifungal screening of the ligand and the complexes

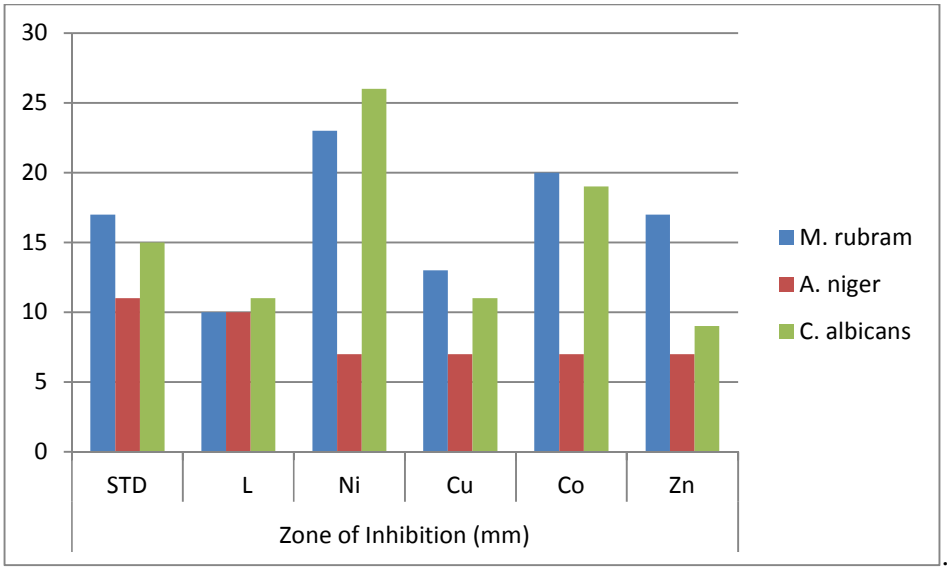

4.2. Anti cancer activity of the single crystal 2, 3-difuryl quinoxaline and its Co(II) complex

In vitro cytotoxicity study was carried out for the ligand and the Co(II) complex against the human breast cancer cell line (MCF 7) by means of a colorimetric micro culture MTT assay which measures mitochondrial dehydrogenase activity as an indication of cell viability. It is evident that the number of cells decreased with an increase in the concentration of the ligand 2, 3-difuryl quinoxaline and complex as shown in Figure 11. The ligand showed moderate activity which is evidenced from low IC_{50} values (50% inhibitory concentration after exposure for 48 h in MTT assay) of 90.19µg/mL and the complex showed a good activity better than the ligand which is evident from the IC_{50} value of 20.25 µg/mL [22-24]. The cytotoxicity results of the ligand and the complex were analysed by means of cell viability curves and expressed with IC50 values in the studied concentration range from 0.1 to 100µM. It is to be noted that the ligands does not show any significant activity (IC_{50}>80 µM) which confirmed that the chelation of the ligands with the cobalt (II) ion is the only responsible factor for the observed cytotoxic property of the complexes.

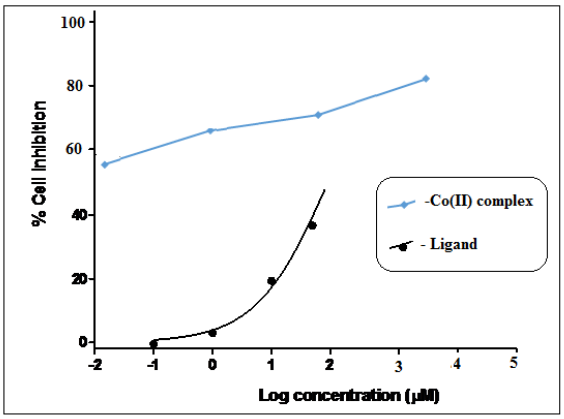

Figure 11. %Growth inhibition of MCF-7 cell line as a function of concentration of the compounds

CONCLUSION

2, 3-difuryl quinoxaline was synthesized and the results of cytotoxic activity and antimicrobial activity data revealed that the compounds possess significant *in vitro* biological activity. The study would be a fruitful matrix for the development of 2,3-difuryl derivatives and its complexes for further bio-evaluation. The structure of the ligand and the complexes were characterized by NMR, IR and elemental analysis data and Single crystal XRD.

Acknowledgement
All authors thank the management of Kongunadu Arts and Science College and PSGR Krishnammal College for Women, Coimbatore for providing research facilities, SAIF STIC Cochin for the analytical data, Department of Biotechnology, KASC, Coimbatore to carry out the biological activities. One of the authors S. J. thanks UGC-Hyderabad (MRP No. 4995/14 (SERO-UGC) for financial support.

REFERENCES

[1] W Guo; H Jin; J Chen; F Chen; J Ding. *J. Braz. Chem. Soc.*, **2009,** 20, 1674-1679.
[2] J Mazumder; R Chakraborty; S Sen; S Vadra; B De; TK Ravi. *Der. Pharm. Chim.*, **2009,** 1, 188-198.
[3]D Shi; G Dou. *Molecules.*, **2008,** 38, 3329-3337.
[4] MA Bogoyevitch; DP Fairlie. *Drug Discovery today.*, **2007,** 16, 622-633.
[5] BV Subba Reddy; L Ramesh; JS Yadav. *Synlett.*, **2011,** 2, 169-172.
[6]J Guillion; P Grellier; M Labaied; P Sonnet; JM Leger; P Dallemagne; N Lemaitre; F Pehourcq; J Rochette; C Sergheraert; C Jarry. *J . Med. Chem.*, **2004,** 47, 1997-2009.
[7] B Debasish; M Sanghamitra; RR Robert; KB Bimal. *Molecules.*, **2010**, 15, 4207-4212.
[8] GM Sheldrick. *Acta Cryst.*, **2008**, A64, 112-122.
[9] OV Dolomanov; LJ Bourhis; RJ Gildea; JAK Howard; HJ Puschmann. *Appl. Cryst.*, **2009,** 42, 339-341.
[10] PJ Crowley; C Lamberth; U Mueller; S Wendeborn; OA Sageot; J Williams; A Bartovic. *Tetrahedron Lett.*, **2010**, 51, 2652–2654.
[11] LM Prescot; JP Harley; KA Donald. Microbiology, 6th ed, McGraw Hill, Manhattan, NY, USA, **2005;** 690–696.
[12] MJ Pelczar; ECS Chan; NR Krig. Text book of Microbiology, 5th edition, Mc Graw-Hill publications, Newyork, 504-508.
[13] WJ Geary. *Co-ord. Chem.Rev.*, **1971,** 7, 81-110.
[14] RS Bhosale; SR Sarda; SS Ardhapure; WN Jadhav; SR Bhusare; RP Pawar. *Tetrahedron Lett.*, **2005**, 46, 7183–7186.
[15] J Jesus Morales-Castallanos; K Hernandez; NS Cromez flores; OR Rodas-Snarez; J Peralta-Cruz. *Molecules.*, **2012,** 17, 5164-5176.
[16] N Raman;YP Raja; A Kulandaisamy. *Proc. Indian Acad. Sci. (Chem. Sci.).*, **2001,** 113, 183-189.
[17] N Raman; S Esthar; CA Thangaraj. *J. Chem. Sci.*, **2004,** 116, 209-213.
[18]N Raman; S Ravichandran, C Thangaraja. *J. Chem. Sci.*, **2004,** 116, 215-219.

[19]AS El-Tabl. *Trans. Met Chem.,* **1998,** 23, 63-65.
[20] MM Li; MMF Ismail; MSA El-Gaby; MA Zahran; YA Ammar. *Molecules.,* **2000,** 5, 864-873.
[21] GP Ouyang; PQ Zhang; GF Xu; BA Song; S Yang; LH Jin; W Xue; DY Hu; P Lu. *Molecules.,* **2006,** 11, 383-392.
[22] SS Karki; R Hazare; S Kumar; VS Bhadauria; J Balzarini; E De Clercq. *Acta Pharm.,* **2009,** 59, 431-440.
[23] A Monks; D Scudiero; P Skehen; R Shoemaker; K Paull; D Vistica; C Hose; J Langley; P Cronise; A Vaigro-Wolff. *J. Natl. Cancer Inst.,* **1991,** 83**,** 757–766.
[24] AA El-Tombary; SA El-Hawash. *Med Chem.,* **2014,** 10(5), 521-32.